J. Fluid Mech. (1990), *vol.* 219, *pp.* 585–607
Printed in Great Britain

Spatial evolution of nonlinear acoustic mode instabilities on hypersonic boundary layers

By M. E. GOLDSTEIN[1] AND D. W. WUNDROW[2]

[1]Lewis Research Center, Cleveland, OH 44135, USA

[2]Sverdrup Technology, Inc., Lewis Research Center, Cleveland, OH 44135, USA

(Received 12 October 1989 and in revised form 30 March 1990)

We consider the effects of strong critical-layer nonlinearity on the spatial evolution of an initially linear 'acoustic mode' instability wave on a hypersonic flat-plate boundary layer. Our analysis shows that nonlinearity, which is initially confined to a thin critical layer, first becomes important when the amplitude of the pressure fluctuations becomes $O(1/M^4 \ln M^2)$, where M is the free-stream Mach number. The flow outside the critical layer is still determined by linear dynamics and therefore takes the form of a linear instability wave – but with its amplitude completely determined by the flow within the critical layer. The latter flow is determined by a coupled set of nonlinear equations, which we had to solve numerically.

1. Introduction

Laminar boundary-layer instabilities are predominantly inviscid at sufficiently high Mach numbers with the so-called vorticity modes exhibiting the most rapid growth at very large Mach numbers (Mack 1984, 1987). The so-called acoustic modes exhibit the most rapid growth at more moderate Mach numbers – with the two-dimensional disturbances growing more rapidly than the corresponding oblique waves.

Mack (1984, 1987) computed the relevant numerical solutions to Rayleigh's equation and Cowley & Hall (1990) worked out the corresponding asymptotic solution for the hypersonic limit where the free-stream Mach number $M \to \infty$. Their results, as well as those of Mack (1984, 1987), suggest that, while the instability wavenumber becomes small, the instability wave growth rate becomes even smaller as $M \to \infty$ which means that there will be a well-defined critical layer in this limit even for the most rapidly growing mode. Nonlinear effects will then balance the resulting singularity at sufficiently large Reynolds numbers and the present work is concerned with extending the Cowley–Hall (1990) analysis into this nonlinear regime.

Boundary-layer-transition experiments often involve spatially growing instability waves generated by relatively two-dimensional, single-frequency excitation devices such as vibrating ribbons or acoustic speakers. As the instability wave propagates downstream, its amplitude continues to increase until nonlinear effects come into play – provided, of course, that the initial amplitude is sufficiently large and/or the mean flow divergence is sufficiently small (i.e. the Reynolds number is sufficiently large).

Our previous remarks suggest that the nonlinearity first comes into play locally in such experiments, i.e. within a critical layer. The appropriate solution to the resulting nonlinear critical-layer problem must then reduce to the linear small

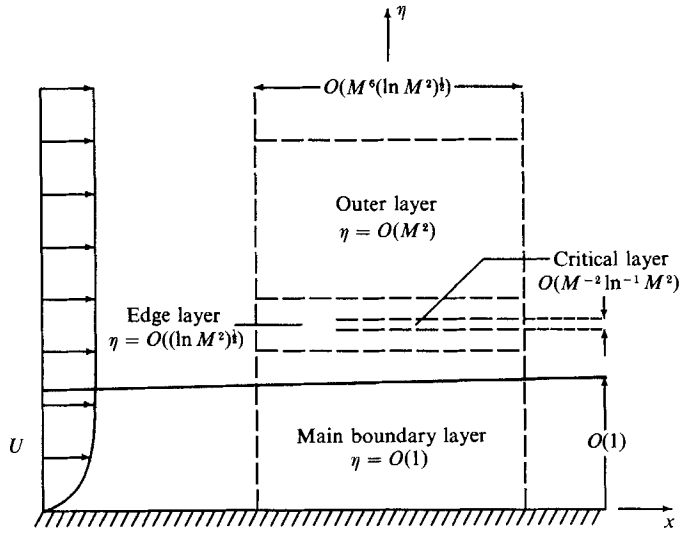

FIGURE 1. Asymptotic structure of high-Mach-number solution.

growth rate hypersonic instability wave solution far upstream in the flow in order to represent the natural downstream continuation of this upstream linear solution. The unsteady flow outside the critical layer continues to behave linearly (i.e. to be representable by a linear instability wave solution) but the corresponding instability wave amplitude is completely determined by the nonlinear dynamics within the critical layer. These considerations fix the relative scaling between instability wave amplitude and Mach number and thereby show that the nonlinearity first becomes important when the pressure fluctuation amplitude becomes $O(1/M^4 \ln M^2)$ in the main boundary layer.

The critical-layer nonlinearity is strong in the sense that it enters through a coefficient in the lowest-order equation (as in the Goldstein, Durbin & Leib 1987 incompressible boundary-layer analysis) rather than through an inhomogeneous higher-order term (as in the Goldstein & Leib 1989 compressible shear-layer analysis). However, it differs from the former analysis (but is similar to the latter) in that critical-layer vorticity and energy equations are now strongly coupled.

But even without this coupling, the present critical-layer vorticity equation would still contain additional nonlinear terms that do not appear in any previous analyses known to the authors. However, we show that the present result can be transformed (along with the energy equation) into the standard (or nearly standard) critical-layer vorticity equation form by a simple change in one of its independent variables. This transformation shows that the additional nonlinearity can be characterized as an unusual type of modulation of the basic critical streamline pattern, which turns out to have a strong effect on the nonlinear vorticity roll-up.

The transformed critical-layer transport equations had to be solved numerically. The computations show that, while nonlinear effects always decrease the instability wave growth in the Goldstein *et al.* (1987) analysis, compressibility effects initially counteract this tendency to produce a dramatic increase in instability wave growth in the present analysis. But this effect is eventually overcome by the usual nonlinear vorticity roll-up, and the instability wave growth rate again tends towards zero.

The overall plan of the paper is as follows. The problem is formulated in §2, where we show how the nonlinear flow gradually evolves from the strictly linear hypersonic

solution. The flow outside the critical layer is a linear inviscid perturbation about a hypersonic (i.e. $M \gg 1$) boundary-layer flow, and is found by extending the asymptotic analysis of Cowley & Hall (1990) into the nonlinear regime. This flow has a triple-layer structure (shown in figure 1) and the solution for the main boundary-layer region is worked out in §3. The critical layer is contained in an adjacent outer region, which we refer to as the 'edge layer', and in §§4 and 5 we obtain the edge-layer solution that applies outside the critical layer. This is then used to formulate the relevant critical-layer problem in §6. The resulting critical-layer vorticity and energy equations are then transformed into the usual nonlinear critical-layer equation form by a suitable change of independent variable. A novel numerical procedure for solving these coupled equations is described in §7. It is based on the method of characteristics and is much more accurate and efficient than the spectral methods used in previous studies. Finally, numerical results are discussed in §8.

2. Formulation

We use the free-stream flow parameters as reference quantities, which are generally denoted by the subscript ∞, and choose the reference length, say Δ to be some suitable boundary-layer thickness (e.g. momentum thickness). Then the steady flow is characterized by the Mach number

$$M \equiv U_\infty / C_\infty, \tag{2.1}$$

and Reynolds number

$$Re \equiv U_\infty \Delta / \nu_\infty, \tag{2.2}$$

where

$$C_\infty = (\gamma \mathscr{R} T_\infty)^{\frac{1}{2}} \tag{2.3}$$

is the speed of sound in the free stream, ν is the kinematic viscosity, γ is the isentropic exponent of the gas, and $\mathscr{R}$ is the gas constant.

We suppose that the flow is two-dimensional and that Re is large enough that the unsteady motion is essentially inviscid and unaffected by mean boundary-layer growth over the region in which nonlinear interaction takes place. We can then suppose that the mean pressure is constant and that the mean flow velocity $U(y)$ depends only on the transverse coordinate y to the required order of approximation.

We shall assume that the variation of viscosity with temperature follows Chapman's approximate law rather than Sutherland's more exact relation. While we realize that these two laws lead to different asymptotic (i.e. high-Mach-number) scalings for the linear-instability-wave solution, we choose to use Chapman's law for the following two reasons: first, the scaled nonlinear solution, which is the primary result of this paper, turns out to be completely independent of the choice of viscosity law, and secondly, Cowley & Hall (1988, 1990) have already published the linear solution for a Chapman's law fluid and are still working on the Sutherland's law result. It would certainly not be very fair to publish the nonlinear Sutherland's law solution before they can get their linear result into print.

We further assume that the wall is insulated and, for simplicity, restrict our attention to an ideal gas with Prandtl number unity. In which case the local mean density R and mean temperature T will be related by

$$RT = 1, \tag{2.4}$$

and the mean velocity and temperature will be given by

$$U = h'(\eta) \tag{2.5}$$

and

$$T = 1 + \tfrac{1}{2}(\gamma - 1) M^2 (1 - U^2), \tag{2.6}$$

respectively, where η is the Dorodnitzyn–Howarth variable (Stewartson 1964) defined by

$$\eta \equiv \int_0^y \frac{\mathrm{d}y}{T}, \tag{2.7}$$

the prime denotes differentiation with respect to η, and h is the Blasius function, i.e. it satisfies

$$hh'' + 2h''' = 0. \tag{2.8}$$

It follows that (Schlichting 1960, pp. 117, 118)

$$U = 1 - \frac{b}{\tilde{\eta}} \mathrm{e}^{-\frac{1}{4}\tilde{\eta}^2} \left[1 - \frac{2}{\tilde{\eta}^2} + O(\tilde{\eta}^{-4}) \right] - \frac{b^2 \mathrm{e}^{-\frac{1}{2}\tilde{\eta}^2}}{\tilde{\eta}^4} + \ldots, \tag{2.9}$$

as $\tilde{\eta} \to \infty$, where

$$\tilde{\eta} \equiv \eta - \beta, \tag{2.10}$$

$\beta \approx 1.73$, and $b \approx 0.462$.

As indicated in § 1, we suppose that the unsteady motion starts as a linear inviscid instability wave (which is governed by Rayleigh's equation) far upstream in the flow. We also suppose that the linear mode is of the acoustic type (Mack 1984, 1987) and that

$$\sigma \equiv \frac{1}{M^2} \ll 1. \tag{2.11}$$

The relevant asymptotic solution to Rayleigh's equation was worked to lowest approximation by Cowley & Hall (1988). They have shown that the scaled complex wavenumber α is $O(\sigma)$, that the phase speed c behaves like

$$c = 1 - \sigma\bar{c} \quad \text{as } \sigma \to 0, \tag{2.12}$$

where $\bar{c} = O(1)$, and that the flow develops a double (actually triple if the free stream is included) layered structure, with a relatively thin outer region, or 'edge layer', where

$$\ln \tilde{Y} \equiv \delta(2\delta - \tilde{\eta}) \tag{2.13}$$

is order unity provided the constant δ satisfies

$$\frac{\mathrm{e}^{-\delta^2}}{2\delta} = \sigma, \tag{2.14}$$

which can be inverted to obtain

$$\delta = \ln^{\frac{1}{2}}(1/\sigma) - \frac{\ln 2 \ln^{\frac{1}{2}}(1/\sigma)}{2 \ln^{\frac{1}{2}}(1/\sigma)} + \ldots.$$

We could, at this point, eliminate δ and carry out the relevant asymptotic expansions in terms of explicit gauge functions involving σ and appropriate combinations of its logarithms. However, it turns out that the resulting formulae will be much simpler if we retain both δ and σ and think of δ as a function of σ (on the same footing as, say, $\ln(1/\sigma)$) which is defined implicitly by (2.14). The relevant asymptotic expansions will then be double power series in σ and δ^{-1}, and possibly their logarithms. But since $O(\sigma) \ll O(\delta^{-1})$, we will often be able to simplify the notation by supposing that the various terms involving δ^{-1} have been incorporated into the coefficients of σ, σ^2, etc. This notational procedure has been used in a number of recent papers on critical layers in order to avoid writing down irrelevant logarithmic terms that play only a passive role in the analysis.

Cowley & Hall (1989) extended their analysis to higher order in σ to show that the instability wave growth rate (or imaginary part of the complex wavenumber) is small relative to $\mathrm{Re}\,\alpha$, or more precisely that

$$\mathrm{Im}\,\alpha = O\left(\frac{\sigma^3}{\delta}\right). \tag{2.15}$$

The linear instability wave will then have a distinct critical layer, which, in view of (2.9), (2.12) and (2.13), must lie in the outer region where $\tilde{Y} = O(1)$, and

$$U = 1-\sigma b\tilde{Y}\left[1-\frac{1}{2\delta^2}(1-\ln\tilde{Y}+\tfrac{1}{2}\ln^2\tilde{Y})+O(\delta^{-3})\right]-\left(\frac{\sigma b\tilde{Y}}{2\delta}\right)^2+\ldots. \tag{2.16}$$

The flow should become nonlinear in this layer because the motion is assumed to be inviscid and the linear instability wave amplitude increases in the downstream direction. The unsteady flow is predominantly linear outside the critical layer and we expect the relevant solution to expand like

$$u = U(\eta)+\epsilon u_1+\epsilon^2 u_2+\ldots \tag{2.17}$$

$$v = \epsilon v_1+\epsilon^2 v_2+\ldots \tag{2.18}$$

$$\theta = T(\eta)+\epsilon\tau_1+\epsilon^2\tau_2+\ldots \tag{2.19}$$

$$p^{1/\gamma} = 1+\epsilon\pi_1+\epsilon^2\pi_2+\ldots, \tag{2.20}$$

where $\{u, v\}$ are the velocity components in the x- and y-directions, θ is the temperature, p is the pressure, and ϵ is a characteristic amplitude of the instability wave in the streamwise region where nonlinearity first becomes important. It will eventually be chosen so that the lowest-order nonlinear terms are of the same order as the linear convection and non-equilibrium terms in the critical-layer vorticity equation. This choice corresponds to a 'distinguished' scaling in which the nonlinear terms are as large as they can be without producing a solution that cannot reduce to the linear solution far upstream in the flow.

The ultimate scaling is, in part, determined by the behaviour of the outer linear solution at the edge of the critical layer. So rather than attempting to give order-of-magnitude arguments to relate ϵ and σ at this point, we choose to wait until the relevant portions of the linear solution are worked out before fixing the ϵ–σ relation. There is little possibility that this temporary two-parameter expansion will promote errors in the analysis because the solution is basically linear outside the critical layer, and the ϵ–σ relation will be fixed before the critical-layer solution is considered.

Then since $\{u_1, v_1, \tau_1, p_1\}$ are determined by linear dynamics, it follows from Goldstein (1984) that the expansion coefficients in (2.17)–(2.20) (which depend on x, η, t and σ) are determined by

$$\mathrm{L}\pi_1 = 0, \tag{2.21}$$

$$\mathrm{L}\pi_2 = \frac{\mathrm{D}}{\mathrm{D}t}\left(\frac{\partial f}{\partial x}+\frac{\partial g}{\partial y}\right)-\frac{2U'}{T}\frac{\partial g}{\partial x}, \tag{2.22}$$

$$\frac{\mathrm{D}}{\mathrm{D}t}u_1+\frac{U'}{T}v_1 = -\sigma\frac{\partial\pi_1}{\partial x}, \tag{2.23}$$

$$\frac{\mathrm{D}}{\mathrm{D}t}(u_2+u_1\pi_1)+\frac{U'}{T}(v_2+v_1\pi_1) = -\sigma T\frac{\partial\pi_2}{\partial x}-f, \tag{2.24}$$

$$\frac{\mathrm{D}v_1}{\mathrm{D}t} = -\sigma T\frac{\partial\pi_1}{\partial y}, \tag{2.25}$$

$$\frac{\mathrm{D}}{\mathrm{D}t}(v_2+v_1\pi_1) = -\sigma T\frac{\partial \pi_2}{\partial y} - g, \tag{2.26}$$

$$\frac{\mathrm{D}}{\mathrm{D}t}\tau_1 + \frac{T'}{T}v_1 = (\gamma-1)\,T\frac{\mathrm{D}\pi_1}{\mathrm{D}t}, \tag{2.27}$$

and a similar equation for τ_2, where the prime still denotes differentiation with respect to η,

$$\mathrm{L} \equiv \frac{\mathrm{D}}{\mathrm{D}t}\left(\frac{\mathrm{D}^2}{\mathrm{D}t^2} - \sigma\boldsymbol{\nabla}\cdot T\boldsymbol{\nabla}\right) + 2\sigma U'\frac{\partial^2}{\partial x\,\partial y}, \tag{2.28}$$

$$\frac{\mathrm{D}}{\mathrm{D}t} \equiv \frac{\partial}{\partial t} + U\frac{\partial}{\partial x}, \tag{2.29}$$

$$\boldsymbol{\nabla} \equiv \frac{\partial}{\partial x}, \frac{\partial}{\partial y}, \tag{2.30}$$

$$f \equiv \frac{\partial}{\partial x}u_1^2 + \frac{\partial}{\partial y}u_1 v_1 + \sigma\tau_1\frac{\partial}{\partial x}\pi_1, \tag{2.31}$$

and

$$g \equiv \frac{\partial}{\partial x}u_1 v_1 + \frac{\partial}{\partial y}v_1^2 + \sigma\tau_1\frac{\partial}{\partial y}\pi_1. \tag{2.32}$$

It now follows from (2.12), (2.15), and the fact that $\alpha = O(\sigma)$ that the solution to (2.21), (2.23), (2.25) and (2.27) that reduces to the upstream linear solution must be of the form

$$u_1 = \frac{\delta}{\sigma}\,\mathrm{Re}\,\Psi_1(\eta, x_1)A^\dagger(x_1)\,\mathrm{e}^{\mathrm{i}\bar{X}}, \tag{2.33}$$

$$v_1 = -\bar{\alpha}\,\mathrm{Re}\,\mathrm{i}\Phi_1(\eta, x_1)A^\dagger \mathrm{e}^{\mathrm{i}\bar{X}}, \tag{2.34}$$

$$\tau_1 = \frac{\delta}{\sigma^2}\,\mathrm{Re}\,\Theta_1 A^\dagger \mathrm{e}^{\mathrm{i}\bar{X}}, \tag{2.35}$$

$$\pi_1 = \mathrm{Re}\,\Pi_1 A^\dagger \mathrm{e}^{\mathrm{i}\bar{X}}, \tag{2.36}$$

where we have put

$$x_1 = \frac{\sigma^3 x}{\delta}, \tag{2.37}$$

$$\bar{X} = \sigma\bar{\alpha}[x-(1-\sigma\bar{c})\,t], \tag{2.38}$$

$(\mathrm{d}A^\dagger/\mathrm{d}x_1 A^\dagger)$, $\bar{\alpha}(\sigma)$, and $\bar{c}(\sigma)$ are real quantities and, to the required level of approximation, Π_1 satisfies Rayleigh's equation

$$\mathscr{L}_1\Pi_1 = 0, \tag{2.39}$$

where

$$\mathscr{L}_n \equiv (U-c)^2\frac{\partial}{\partial\eta}\frac{1}{(U-c)^2}\frac{\partial}{\partial\eta} - (n\alpha)^2 T\left[T - \frac{1}{\sigma}(U-c)^2\right] \quad \text{for } n = 1, 2, \ldots \tag{2.40}$$

are the linear Rayleigh operators, the complex wavenumber and phase speed α and c, respectively, are given by

$$\alpha = \sigma\bar{\alpha} + \frac{\sigma^3}{\delta}\frac{A^{\dagger\prime}}{\mathrm{i}A^\dagger}, \tag{2.41}$$

$$c = 1 - \sigma\bar{c} - \frac{\sigma^2}{\delta\bar{\alpha}}\frac{A^{\dagger\prime}}{\mathrm{i}A^\dagger}, \tag{2.42}$$

and the prime now denotes differentiation with respect to x_1. We note in passing that $\bar{\alpha}$ has an expansion of the form

$$\bar{\alpha} = \bar{\alpha}_1 + \sigma\bar{\alpha}_2 + \sigma^2\bar{\alpha}_3 + \ldots, \tag{2.43}$$

where each of the coefficients has its own series expansion in δ^{-1}, $(\ln\delta)^{-\frac{1}{2}}$, etc. (see (2.14)) and similarly for $\bar{c}$, i.e.

$$\bar{\alpha}_n = \bar{\alpha}_n^{(0)} + \frac{1}{\delta}\bar{\alpha}_n^{(1)} + \ldots, \tag{2.44}$$

$$\bar{c}_n = \bar{c}_n^{(0)} + \frac{1}{\delta}\bar{c}_n^{(1)} + \ldots. \tag{2.45}$$

Π_1 must satisfy the boundary conditions

$$\frac{\partial\Pi_1}{\partial\eta} = 0 \quad \text{at } \eta = 0, \tag{2.46}$$

$$\Pi_1 \to 0 \quad \text{as } \eta \to \infty \tag{2.47}$$

and, in order to be consistent with the linear solution far upstream, we must require that

$$A^\dagger \to a\exp(\kappa x_1) \quad \text{as } x_1 \to -\infty, \tag{2.48}$$

where κ is the scaled growth rate of the upstream linear instability wave and a is a complex constant. Finally, the remaining functions of η and x_1, i.e. Ψ_1, Φ_1, and Θ_1 can readily be found from (2.23), (2.25) and (2.27) once Π_1 is known.

In the following two sections we extend the results of this section to derive dispersion relations for the external instability wave amplitude.

3. Linear solution in main boundary layer

First suppose that $\eta = O(1)$. It is easy to see from the Cowley–Hall (1988) analysis that Π_1 should expand like

$$\Pi_1 = \frac{1}{\sigma}(P_0 + \sigma P_1 + \sigma^2 P_2 + \ldots), \tag{3.1}$$

where each of the expansion coefficients in turn has the expansion

$$P_n = P_n^{(0)} + \frac{1}{\delta}P_n^{(1)} + \frac{1}{\delta^2}P_n^{(2)} + \ldots \quad \text{for } n = 1, 2, \ldots. \tag{3.2}$$

Substituting these into (2.39) and equating coefficients of like powers of σ and δ, we find that

$$\mathscr{L}_1^{(0)}P_0 = 0, \tag{3.3}$$

$$\mathscr{L}_1^{(0)}P_1^{(0)} = Q_1\frac{(1-U)^2}{P_0} \equiv \bar{\alpha}_1(\gamma-1)(1-U^2)\left\{\left[\tfrac{1}{2}(\gamma-1)(1-U^2)-(U-1)^2\right]\bar{\alpha}_2 + \left[1-\frac{1}{\gamma-1}\left(\frac{1-U}{1+U}\right)+\bar{c}_1(1-U)\right]\bar{\alpha}_1\right\}P_0 - \frac{2\bar{c}_1U'}{(1-U)^2}\frac{\mathrm{d}P_0}{\mathrm{d}\eta}, \tag{3.4}$$

and

$$\mathscr{L}_1^{(0)}P_2^{(1)} = Q_2\frac{(1-U)^2}{P_0}, \tag{3.5}$$

where

$$Q_2 \equiv Q_{2r} - \mathrm{i}q\frac{A^{\dagger\prime}}{A^\dagger}, \tag{3.6}$$

Q_{2r}, q are real,

$$q \equiv (\gamma-1)(1+U)\bar{\alpha}_1[\tfrac{1}{2}(\gamma-1)(1+U)+U]P_0^2 - \frac{U'}{\bar{\alpha}_1(1-U)^4}\frac{\mathrm{d}P_0^2}{\mathrm{d}\eta}, \tag{3.7}$$

and we have put

$$\mathscr{L}_1^{(0)} \equiv (1-U)^2\frac{\mathrm{d}}{\mathrm{d}\eta}\frac{1}{(U-1)^2}\frac{\mathrm{d}}{\mathrm{d}\eta} - \bar{\alpha}_1^2(\tfrac{1}{2}(\gamma-1))(1-U^2)[\tfrac{1}{2}(\gamma-1)(1-U^2)-(U-1)^2]. \tag{3.8}$$

Equation (3.3) was solved numerically by Cowley & Hall (1988). They point out that

$$P_0 \sim \frac{D}{\bar{\eta}^3}\mathrm{e}^{-\frac{1}{2}\bar{\eta}^2} \quad \text{as } \eta \to \infty, \tag{3.9}$$

where D is an, as yet, undetermined constant. Equations (3.4) and (3.5) can now be solved by variation of parameters to obtain

$$P_1^{(0)} = P_0\int\left(\frac{1-U}{P_0}\right)^2\int_0^\eta Q_1(\hat{\eta})\,\mathrm{d}\hat{\eta}\,\mathrm{d}\eta, \tag{3.10a}$$

$$P_2^{(1)} = P_0\int\left(\frac{1-U}{P_0}\right)^2\int_0^\eta Q_2(\hat{\eta})\,\mathrm{d}\hat{\eta}\,\mathrm{d}\eta. \tag{3.10b}$$

It follows that

$$P_1^{(0)} \sim \frac{b^2}{D}\int_0^\infty Q_1\,\mathrm{d}\eta, \quad P_2^{(1)} \sim \frac{b^2}{D}\int_0^\infty Q_2\,\mathrm{d}\eta \quad \text{as } \eta\to\infty. \tag{3.11a, b}$$

4. Linear solution in the edge layer

Cowley & Hall (1988) point out that the expansion (3.1) breaks down at large distances from the wall and then proceed to construct a new 'outer' solution for the region where $\tilde{Y} = O(1)$ (see (2.13)). The expansion in this region, which we refer to as the 'edge layer' (see figure 1), must be of the form

$$\Pi_1 = 1+\left(\frac{\sigma}{\delta}\right)\tilde{P}_1+\left(\frac{\sigma}{\delta}\right)^2\tilde{P}_2+\ldots, \tag{4.1}$$

where again each expansion coefficient has its own series expansion

$$\tilde{P}_n = \delta^2\tilde{P}_n^{(-2)}+\delta\tilde{P}_n^{(-1)}+\tilde{P}_n^{(0)}+\frac{1}{\delta}\tilde{P}_n^{(1)}+\ldots \tag{4.2}$$

in terms of δ^{-1}, $\ln\delta$, etc. Substituting this, together with the new variable (2.13), into (2.39), equating coefficients of (σ/δ) and saving only essential terms, we find upon integration that

$$\tilde{P}_1^{(-1)} = \tilde{E}_1^{(-1)},$$

$$\tilde{P}_1^{(0)} = \tilde{B}_1^{(0)}(\tfrac{1}{2}b^2\tilde{Y}^2-2\bar{c}_1 b\tilde{Y}+\bar{c}_1^2\ln\tilde{Y})+\tilde{E}_1^{(0)}, \tag{4.3}$$

$$\begin{aligned}\tilde{P}_2^{(0)} = {} & \left[\frac{\bar{\alpha}_1^2}{\bar{c}_1}T_c^2+2\left(\bar{c}_2^{(1)}+\frac{1}{\bar{\alpha}_1}\frac{A^{\dagger\prime}}{\mathrm{i}A^\dagger}\right)\tilde{B}_1^{(0)}\right](\bar{c}_1\ln\tilde{Y}-b\tilde{Y}) \\ & +\frac{\bar{\alpha}_1^2}{\bar{c}_1^2}\left\{b\int_0^Y(b\tilde{Y}-2\bar{c}_1)\ln\tilde{Y}\,\mathrm{d}\tilde{Y}+\tfrac{1}{2}\bar{c}_1^2\ln^2\tilde{Y}-[1-\bar{c}_1^2(\gamma-1)^2]\right. \\ & \left.\times\int\frac{(b\tilde{Y}-c_1)^2}{\tilde{Y}}[\phi^\pm+\ln|b\tilde{Y}-\bar{c}_1|]\,\mathrm{d}\tilde{Y}\right\} \\ & +\tilde{B}_2^{(0)}(\tfrac{1}{2}b^2\tilde{Y}^2-2\bar{c}_1 b\tilde{Y}+\bar{c}_1^2\ln\tilde{Y})+\tilde{E}_2^{(0)},\end{aligned} \tag{4.4}$$

where we note that the lowest-order solution (i.e. $\tilde{P}_1$) is given in Cowley & Hall (1988), $\tilde{B}_1$, $\tilde{E}_1$, $\tilde{E}_2$, and $\phi^{\pm}$ are constants of integration (the latter of which can be different depending on whether $\tilde{Y} \gtrless \bar{c}_1/b$) and

$$T_c \equiv 1+(\gamma-1)\,\bar{c}_1 \tag{4.5}$$

is the mean temperature at the critical level where

$$b\tilde{Y} = \bar{c}_1. \tag{4.6}$$

This solution does not satisfy appropriate free-stream boundary conditions and it is necessary to introduce an outer region where the variable

$$\hat{\eta} \equiv \sigma\eta \tag{4.7}$$

is order one (see figure 1). The solution in this region is

$$\Pi_1 = (1+\sigma\hat{B}_1)\exp\left(-\bar{\alpha}(1-\sigma\bar{c}_1^2)^{\frac{1}{2}}\hat{\eta}\right)+\ldots \tag{4.8}$$

to the required order of accuracy and matching with (4.1) shows that

$$\tilde{B}_1^{(0)} = \frac{\bar{\alpha}_1}{\bar{c}_1^2}, \tag{4.9}$$

and

$$\tilde{E}_1^{(0)} = \bar{\alpha}_1\{T_c^2-[1-\bar{c}_1^2(\gamma-1)^2][\phi^- + \ln|\bar{c}_1|]\}+\frac{2}{\bar{c}_1}\left(\bar{c}_2^{(1)}+\frac{1}{\bar{\alpha}_1}\frac{A^{\dagger\prime}}{\mathrm{i}A^{\dagger}}\right)+\frac{\bar{c}_1^2}{\bar{\alpha}_1}\tilde{B}_2^{(0)}. \tag{4.10}$$

Finally, matching (3.1) and (4.1) and using (3.9) and (3.11) shows that

$$D = \frac{b^2\bar{\alpha}_1}{\bar{c}_1^2}, \tag{4.11}$$

$$1 = \frac{\bar{c}_1^2}{\bar{\alpha}_1}\int_0^{\infty} Q_1\,\mathrm{d}\eta, \tag{4.12}$$

$$\operatorname{Im}\phi^+ = 0, \tag{4.13}$$

$$\tilde{B}_2^{(0)} = \left(\frac{\bar{\alpha}_1}{\bar{c}_1}\right)^2[1-\bar{c}_1^2(\gamma-1)^2](\ln|b|+\phi^+), \tag{4.14}$$

and

$$\bar{\alpha}_1^2\bar{c}_1[1-\bar{c}_1^2(\gamma-1)^2]\operatorname{Im}\phi^- + 2\frac{A^{\dagger\prime}}{A^{\dagger}} = \bar{c}_1^3\frac{A^{\dagger\prime}}{A^{\dagger}}\int_0^{\infty} q\,\mathrm{d}\eta. \tag{4.15}$$

Having obtained the final solution for Π_1, we now proceed to write down the formulae for the other physical quantities. However, we need only determine their limiting forms as $\tilde{Y}\to\bar{c}_1/b$. Thus, substituting (2.13), (2.34), (2.36), (2.41), (2.42), (4.3) and (4.4) into (2.25) and equating coefficients of like powers of σ, we find

$$\Phi_1 = \frac{\bar{\alpha}_1(\bar{c}-b\tilde{Y})}{(\bar{\alpha}\bar{c}_1)^2}+\left(\frac{\sigma}{\delta}\right)\frac{1}{\bar{c}_1}\left(T_c^2+\frac{1}{\bar{\alpha}_1^2\bar{c}_1}\frac{A^{\dagger\prime}}{\mathrm{i}A^{\dagger}}\right)+\ldots, \tag{4.16}$$

where $\bar{c}$ can contain higher-order terms in σ and the dots indicate that higher-order terms in $(\bar{c}-bY)$ as well as in σ have been omitted. Substituting this together with (2.33) and the previous equations into (2.23) and using (2.9)

$$\Psi_1 = \frac{\bar{\alpha}_1}{T(\bar{\alpha}\bar{c}_1)^2}(b\tilde{Y}+\ldots)+\frac{\sigma}{\delta}\left\{\frac{T}{(\bar{c}_1-b\tilde{Y})}\left[\frac{b\tilde{Y}}{\bar{c}_1}\left(\frac{T_c}{T}\right)^2-1\right]\right.$$
$$\left.+\frac{b\tilde{Y}}{T\bar{c}_1^2}\left[\ln\tilde{Y}-[1-\bar{c}_1^2(\gamma-1)^2]\left(\phi^{\pm}-\phi^+ + \ln\left|\tilde{Y}-\frac{\bar{c}_1}{b}\right|\right)\right]\right\}+\ldots \quad \text{for } \tilde{Y}\gtrless\frac{\bar{c}_1}{b}. \tag{4.17}$$

And finally, proceeding similarly with (2.35) and (2.27), we obtain

$$\Theta_1 = -\frac{\bar{\alpha}_1(\gamma-1)}{T(\bar{\alpha}\bar{c}_1)^2} b\tilde{Y} + \ldots. \tag{4.18}$$

5. Nonlinear edge-layer terms

The lowest approximation (in terms of σ) of the $O(\epsilon^2)$ terms in the expansions (2.17)–(2.20) has to be determined before the solution within the critical layer can be found. However, it is only necessary to consider the edge-layer solution for this purpose. It follows from (2.33)–(2.36) that this solution must be of the form

$$\pi_2 = \Pi_2^{(0)} + \mathrm{Re}\,\Pi_2^{(2)} \mathrm{e}^{2\mathrm{i}\bar{X}}, \tag{5.1}$$

$$v_2 + v_1\pi_1 = -2\bar{\alpha}[\Phi_2^{(0)} + \mathrm{Re}\,\mathrm{i}\Phi_2^{(2)} \mathrm{e}^{2\mathrm{i}\bar{X}}], \tag{5.2}$$

and

$$u_2 + u_1\pi_1 = \frac{\delta}{\sigma}[\Psi_2^{(0)} + \mathrm{Re}\,\Psi_2^{(2)} \mathrm{e}^{2\mathrm{i}\bar{X}}], \tag{5.3}$$

where the, as yet, unknown coefficients are functions of η, x_1, and σ. Substituting (5.1) into (2.22) and using (2.31), (2.28)–(2.36) and (2.40), we find

$$\mathscr{L}_2 \Pi_2^{(2)} = -\frac{1}{\sigma}\left\{2\mathrm{i}\alpha TF + (U-c)^2 \frac{\partial}{\partial\eta}\left[\frac{G}{(U-c)^2}\right]\right\}, \tag{5.4}$$

where

$$F \equiv \tfrac{1}{2}\mathrm{i}\alpha\left(\frac{\delta}{\sigma}\right)^2\left[2\Psi_1^2 - \frac{1}{T\delta}\frac{\partial}{\partial\eta}(\Phi_1\Psi_1) + \frac{\sigma}{\delta}\Theta_1\Pi_1\right]A^{\dagger 2}, \tag{5.5}$$

and

$$G \equiv \frac{1}{2}\frac{\delta}{\sigma^2}\left(2\alpha^2\Phi_1\Psi_1 - \frac{\alpha^2}{\delta T}\frac{\partial}{\partial\eta}\Phi_1^2 + \sigma\frac{\Theta_1}{T}\frac{\partial\Pi_1}{\partial\eta}\right)A^{\dagger 2}. \tag{5.6}$$

Substituting (2.6), (2.13), (2.16), (2.40)–(2.43) and (4.1), (4.3) and (4.16)–(4.18) into this result we find that

$$\tilde{Y}(\bar{c}_1 - b\tilde{Y})^2 \frac{\partial}{\partial\tilde{Y}}\frac{\tilde{Y}}{(\bar{c}_1-b\tilde{Y})^2}\frac{\partial\Pi_2^{(2)}}{\partial\tilde{Y}} = \frac{A^{\dagger 2}}{\sigma\bar{c}_1^4}\left[\frac{b\tilde{Y}}{T}\left(b\tilde{Y} + \frac{\bar{c}_1 - b\tilde{Y}}{T}\right) - \tfrac{1}{2}b\tilde{Y}(\gamma-1)(\bar{c}_1-b\tilde{Y})^2\frac{\mathrm{d}}{\mathrm{d}\tilde{Y}}\frac{\tilde{Y}}{T^2}\right] \tag{5.7}$$

to lowest approximation in σ when $\tilde{Y} = O(1)$. It follows that

$$\tilde{Y}\frac{\partial\Pi_2^{(2)}}{\partial\tilde{Y}} = \frac{(\bar{c}_1 - b\tilde{Y})A^{\dagger 2}}{\sigma\bar{c}_1^3 T_c}[1 + O(\bar{c}_1 - b\tilde{Y})] \quad \text{as } \tilde{Y} \to \frac{\bar{c}_1}{b}. \tag{5.8}$$

It therefore follows from (2.13), (2.16), (2.26), (5.2) and (5.6) that

$$\Phi_2^{(2)} = \frac{\delta}{\sigma^2}\frac{A^{\dagger 2}}{4T_c\bar{c}_2^3\bar{\alpha}^2}[1 + O(\bar{c}_1 - b\tilde{Y})] \quad \text{as } \tilde{Y} \to \frac{\bar{c}_1}{b}, \tag{5.9}$$

and similarly from (2.24), (5.3) and (5.5) that

$$\Psi_2^{(2)} = -\frac{\delta}{\sigma^2}A^{\dagger 2}[J_1 + O(b\tilde{Y} - \tilde{c}_1)] \quad \text{as } \tilde{Y} \to \frac{\bar{c}_1}{b}, \tag{5.10}$$

where J_1 is an $O(1)$ constant.

6. The critical layer

Equation (4.17) shows that the edge-layer solution becomes singular in the critical layer where $\tilde{Y} = b/\bar{c}_1$ (see figure 1). The governing equations therefore have to be rescaled to obtain a bounded result in this region. The thickness of the linear small-growth-rate critical layer is of the order of that growth rate divided by the mean velocity gradient times the real part of the wavenumber, i.e.

$$O\left(\frac{\left(\frac{\sigma^3}{\delta}\right)}{(\sigma\delta)\,\sigma}\right) = O\left(\frac{\sigma}{\delta^2}\right).$$

It therefore follows from (2.10) and (2.13) that the appropriate transverse coordinate in this region is

$$\bar{Y} \equiv \left(\tilde{Y} - \frac{\bar{c}_1}{b}\right)\frac{\delta}{\sigma}. \tag{6.1}$$

Equations (2.16)–(2.20), (2.33)–(2.36), (4.1), (4.16), (4.17), (5.1)–(5.3) and (5.8)–(5.10) suggest that the flow in this region should expand like

$$u = 1 - \sigma(b+\ldots)\frac{\bar{c}_1}{b} - \frac{\sigma^2}{\delta}b\bar{Y} - \left(\frac{\sigma\bar{c}_1}{2\delta}\right)^2 + \frac{\epsilon\delta}{\sigma}\frac{\mathrm{Re}\,A^\dagger \mathrm{e}^{\mathrm{i}\bar{X}}}{T_c\,\bar{\alpha}_1\,\bar{c}_1} + \epsilon\bar{u}_1 + \frac{\delta^2\epsilon^2}{\sigma^3}\bar{u}_2 + \ldots, \tag{6.2}$$

$$\bar{v} = \frac{\epsilon\delta}{\sigma}\mathrm{Re}\left[\left(\frac{b\bar{Y}}{\bar{c}_1^2} - \frac{\bar{\alpha}T_c^2}{\bar{c}_1}\right)\mathrm{i}A^\dagger - \frac{1}{\bar{c}_1^2\,\bar{\alpha}_1}A^{\dagger\prime}\right]\mathrm{e}^{\mathrm{i}\bar{X}} - \frac{\delta^3\epsilon^2}{\sigma^4}\frac{1}{2\bar{\alpha}\bar{c}_1^3\,T_c}\mathrm{Re}\,\mathrm{i}A^{\dagger 2}\mathrm{e}^{2\mathrm{i}\bar{X}} + \epsilon\bar{v}_1 + \ldots \tag{6.3}$$

$$\theta = T_c + \frac{\sigma}{\delta}(\gamma-1)\,b\tilde{Y} + \frac{\epsilon\delta}{\sigma^2}\bar{\tau}_1 + \ldots, \tag{6.4}$$

and

$$p^{1/\gamma} = 1 + \epsilon\,\mathrm{Re}\,A^\dagger \mathrm{e}^{\mathrm{i}\bar{X}} + \frac{\epsilon\sigma}{\delta}\bar{\pi}_1 + \ldots, \tag{6.5}$$

where the passive terms involving $\ln(\sigma/\delta)$ have been incorporated into $\bar{u}_1$, etc., and

$$\bar{v} \equiv v\left(\frac{\delta}{\sigma}\right)^2. \tag{6.6}$$

Then the critical-layer solution will match with the 'outer' edge-layer solution if we require that

$$\bar{\tau}_1 \to -\frac{(\gamma-1)}{T_c\,\bar{\alpha}_1\,\bar{c}_1}\mathrm{Re}\,A^\dagger \mathrm{e}^{\mathrm{i}\bar{X}}, \tag{6.7}$$

$$\frac{\partial\bar{u}_1}{\partial\bar{Y}} \to \frac{b}{\bar{\alpha}_1(T_c\,\bar{c}_1)^2}\mathrm{Re}\,A^\dagger \mathrm{e}^{\mathrm{i}\bar{X}}, \tag{6.8}$$

as

$$\bar{Y} \to \pm\infty,$$

and

$$\Delta\bar{u}_1 \equiv \lim_{\bar{Y}\to\infty}\left[\bar{u}_1(\bar{Y}) - \bar{u}_1(-\bar{Y})\right] = -\frac{1-\bar{c}_1^2(\gamma-1)^2}{T_c\,\bar{c}_1}\mathrm{Re}\,(\phi^+ - \phi^-)\,A^\dagger \mathrm{e}^{\mathrm{i}\bar{X}} + \text{higher harmonics}. \tag{6.9}$$

The expansion coefficients $\bar{u}_1$, $\bar{v}_1$, $\bar{\tau}_1$, etc. are functions of X, $\bar{Y}$ and x_1 only. They

are determined by the inviscid vorticity, energy and continuity equations, which can be written as

$$\bar{D}\omega-\frac{\omega}{\gamma p}\bar{D}p=\frac{\delta^2\tilde{Y}}{T\gamma p}\left[\left(\bar{\alpha}\theta_{\bar{X}}+\frac{\sigma^2}{\delta}\theta_{x_1}\right)P_{\bar{Y}}-\theta_{\bar{Y}}\left(\bar{\alpha}p_{\bar{X}}+\frac{\sigma^2}{\delta}p_{x_1}\right)\right], \tag{6.10}$$

and

$$\frac{1}{\gamma p}\bar{D}p=\frac{1}{(\gamma-1)\theta}\bar{D}\theta=-\left(\bar{\alpha}u_{\bar{X}}-\frac{\tilde{Y}}{T}\bar{v}_{\bar{Y}}+\frac{\sigma^2}{\delta}u_{x_1}\right), \tag{6.11a, b}$$

where we have put

$$\bar{D}\equiv\bar{\alpha}(u-c)\frac{\partial}{\partial\bar{X}}-\bar{v}\frac{\tilde{Y}}{T}\frac{\partial}{\partial\bar{Y}}+\frac{\sigma^2}{\delta}u\frac{\partial}{\partial x_1}, \tag{6.12}$$

and

$$\omega=\frac{\delta^2}{\sigma}\frac{\tilde{Y}}{T}\frac{\partial u}{\partial\bar{Y}}+\frac{\sigma^3}{\delta^2}\left(\bar{\alpha}\frac{\partial\bar{v}}{\partial\bar{X}}+\frac{\sigma^2}{\delta}\bar{v}_{x_1}\right) \tag{6.13}$$

is the vorticity.

The crucial step in the analysis is to choose the relation between the amplitude scale ϵ and the wavelength scale σ so that the nonlinear terms produce a critical-layer velocity jump of the same order as the velocity jump due to linear effects, i.e. $O(\epsilon)$. A little experimentation shows that nonlinear effects will influence the $O(\epsilon)$ term in u (through both the streamwise and transverse convection terms in $\bar{D}$ as well as the vorticity source term on the right-hand side of (6.10)) if we take

$$\epsilon=\frac{\sigma^3}{\delta^2}. \tag{6.14}$$

Then $\bar{u}_1$ and $\bar{\tau}_1$ will satisfy

$$\bar{\mathscr{D}}\left(\frac{\partial\bar{u}_1}{\partial\bar{Y}}-\frac{b^2\bar{Y}}{T_c\bar{c}_1}\right)=-\bar{\alpha}\left[\frac{\partial\bar{\tau}_1}{\partial\bar{Y}}+b(\gamma-1)\right]\mathrm{Re}\,\mathrm{i}A^\dagger\mathrm{e}^{\mathrm{i}\bar{X}}, \tag{6.15}$$

and

$$\bar{\mathscr{D}}(\bar{\tau}_1+b(\gamma-1)\,\bar{Y})=0, \tag{6.16}$$

where we have put

$$\bar{\mathscr{D}}\equiv\frac{\partial}{\partial x_1}-\bar{\alpha}\left(b\bar{Y}-\frac{1}{T_c\bar{\alpha}\bar{c}_1}\mathrm{Re}\,A^\dagger\mathrm{e}^{\mathrm{i}\bar{X}}\right)\frac{\partial}{\partial\bar{X}}$$
$$-\frac{1}{T_c}\left\{\mathrm{Re}\left[\left(\frac{\bar{Y}}{\bar{c}_1}-\frac{\bar{\alpha}T_c^2}{b}-\frac{1}{bT_c\bar{\alpha}\bar{c}_1^2}\mathrm{Re}\,A^\dagger\mathrm{e}^{\mathrm{i}\bar{X}}\right)\mathrm{i}A^\dagger-\frac{1}{\bar{c}_1 b\bar{\alpha}_1}A^{\dagger\prime}\right]\mathrm{e}^{\mathrm{i}\bar{X}}\right\}\frac{\partial}{\partial\bar{Y}}. \tag{6.17}$$

This can be greatly simplified and put into a more standard form by taking x_1, $\bar{X}$, and

$$\bar{Y}_0\equiv-\bar{Y}+\frac{1}{bT_c\bar{\alpha}_1\bar{c}_1}\mathrm{Re}\,A^\dagger\mathrm{e}^{\mathrm{i}\bar{X}} \tag{6.18}$$

as new independent variables, in which case $\bar{\mathscr{D}}$ becomes

$$\bar{\mathscr{D}}=\frac{\partial}{\partial x_1}+\bar{\alpha}b\bar{Y}_0\frac{\partial}{\partial\bar{X}}-\frac{T_c\bar{\alpha}_1}{b}(\mathrm{Re}\,\mathrm{i}A^\dagger\mathrm{e}^{\mathrm{i}\bar{X}})\frac{\partial}{\partial\bar{Y}_0}. \tag{6.19}$$

It now follows from (3.5), (4.13), (4.15) and (6.9) that

$$\frac{1}{\pi}\int_0^{2\pi}\int_{-\infty}^{\infty}\mathrm{e}^{-\mathrm{i}\bar{X}}\frac{\partial\bar{u}_1}{\partial\bar{Y}_0}\mathrm{d}\bar{Y}_0\,\mathrm{d}\bar{X}=-\frac{\mathrm{i}}{\bar{c}_1\bar{\alpha}_1\Gamma}A^{\dagger\prime}, \tag{6.20}$$

where we have put

$$\frac{1}{\Gamma}\equiv-\frac{1}{T_c\bar{c}_1\bar{\alpha}_1}\left(2-\bar{c}_1^3\int_0^{\infty}q\,\mathrm{d}\eta\right), \tag{6.21}$$

To reduce the number of parameters and thereby put these results in a more universal form, we introduce the new renormalized variables

$$H \equiv \frac{1}{(\gamma-1)\,\Gamma}\left[\bar{\tau}_1+\frac{\gamma-1}{T_c\,\bar{\alpha}_1\,\bar{c}_1}\operatorname{Re} A^{\dagger}\mathrm{e}^{\mathrm{i}\bar{X}}\right], \tag{6.22}$$

$$\Omega \equiv -\frac{T_c\,\bar{c}_1}{b\Gamma}\left[\frac{\partial \bar{u}_1}{\partial \bar{Y}_0}+\frac{b}{\bar{\alpha}_1(T_c\,\bar{c}_1)^2}\operatorname{Re} A^{\dagger}\mathrm{e}^{\mathrm{i}\bar{X}}\right], \tag{6.23}$$

$$A \equiv \frac{T_c A^{\dagger}\exp(\mathrm{i}X_0)}{\Gamma^2}, \tag{6.24}$$

$$Y \equiv \frac{b\bar{Y}_0}{\Gamma}, \tag{6.25}$$

$$X \equiv \bar{X}-X_0, \tag{6.26}$$

and

$$\bar{x} \equiv \Gamma\bar{\alpha}_1 x_1 - x_0. \tag{6.27}$$

Then H and Ω satisfy the homogeneous boundary conditions

$$H, \Omega \to 0 \quad \text{as } Y \to \pm\infty, \tag{6.28}$$

and (6.15), (6.16), (6.19) and (6.20) become

$$\mathscr{D}\Omega = \left(1-r+r\frac{\partial H}{\partial Y}\right)\operatorname{Re}\mathrm{i}A\,\mathrm{e}^{\mathrm{i}X}, \tag{6.29}$$

$$\mathscr{D}H = -\operatorname{Re}\mathrm{i}A\,\mathrm{e}^{\mathrm{i}X}, \tag{6.30}$$

and

$$\frac{1}{\pi}\int_{-\infty}^{\infty}\int_{0}^{2\pi}\Omega\,\mathrm{e}^{-\mathrm{i}X}\,\mathrm{d}Y\,\mathrm{d}X = \mathrm{i}\frac{\mathrm{d}A}{\mathrm{d}\bar{x}}, \tag{6.31}$$

where we have put

$$\mathscr{D} \equiv \frac{\partial}{\partial \bar{x}}+Y\frac{\partial}{\partial X}-(\operatorname{Re}\mathrm{i}A\,\mathrm{e}^{\mathrm{i}X})\frac{\partial}{\partial Y} \tag{6.32}$$

and

$$r \equiv (\gamma-1)\,\bar{c}_1 = T_c-1. \tag{6.33}$$

Since $A \to 0$ as $\bar{x} \to -\infty$ these equations imply that

$$H \to -\operatorname{Re}\frac{A\,\mathrm{e}^{\mathrm{i}X}}{Y-\mathrm{i}\bar{\kappa}}, \tag{6.34}$$

and

$$\Omega \to (1-r)\operatorname{Re}\frac{A\,\mathrm{e}^{\mathrm{i}X}}{Y-\mathrm{i}\bar{\kappa}} \tag{6.35}$$

when

$$A \to \mathrm{e}^{\bar{\kappa}\bar{x}} \quad \text{as } \bar{x} \to -\infty, \tag{6.36}$$

where

$$\bar{\kappa} \equiv (1-r)\,\pi \tag{6.37}$$

is the scaled (and normalized) linear growth rate. The solution to these equations can therefore be made to satisfy the upstream matching condition (2.48) if we choose the, as yet, unspecified real constants X_0 and x_0 to be

$$X_0 = -\arg a, \tag{6.38}$$

and

$$x_0 = \frac{1}{\bar{\kappa}}\ln\frac{\Gamma^2}{|a|\,T_c}. \tag{6.39}$$

7. Numerical computations

The coupled nonlinear evolution equations (6.29)–(6.31) must be solved numerically. It is easy to see from these equations and the upstream boundary condition (6.36) that the solution A will remain real for all values of $\bar{x}$. The problem is most easily solved by introducing the Lagrangian coordinates, say X_0, Y_0 via

$$\frac{\mathrm{d}X}{\mathrm{d}\bar{x}} = Y, \tag{7.1}$$

$$\frac{\mathrm{d}Y}{\mathrm{d}\bar{x}} = A(\bar{x})\sin X, \tag{7.2}$$

where $$X_0 \equiv X|_{\bar{x}=\bar{x}_0}, Y_0 \equiv Y|_{\bar{x}=\bar{x}_0} \quad \text{as } \bar{x}_0 \to -\infty. \tag{7.3}$$

Then it is easy to show that

$$\frac{\partial(X, Y)}{\partial(X_0, Y_0)} = 1, \tag{7.4}$$

and consequently that (6.29) and (6.30) can be written as

$$\frac{\mathrm{d}H}{\mathrm{d}\bar{x}} = A(\bar{x})\sin X \tag{7.5}$$

and

$$\frac{\mathrm{d}\Omega}{\mathrm{d}\bar{x}} = \left[r - 1 - r\frac{\partial(X, H)}{\partial(X_0, Y_0)}\right] A \sin X. \tag{7.6}$$

Comparing (7.5) and (7.2) shows that

$$H = Y + F(X_0, Y_0), \tag{7.7}$$

where F depends only on X_0 and Y_0, and it follows from (6.34), (6.36) and (7.3) that

$$F = -Y_0 - A(\bar{x}_0)\,\mathrm{Re}\frac{\exp(\mathrm{i}X_0)}{Y_0 - \mathrm{i}\bar{\kappa}}, \tag{7.8}$$

where $$A(\bar{x}_0) = \exp(\bar{\kappa}\bar{x}_0). \tag{7.9}$$

Hence $F \approx -Y_0$, and (7.6) can therefore be written as

$$\frac{\mathrm{d}\Omega}{\mathrm{d}\bar{x}} = -\left(1 - r\frac{\partial X}{\partial X_0}\right) A \sin X. \tag{7.10}$$

Finally, (7.4) shows that (6.3) can be written as

$$\frac{1}{\pi}\int_{-\infty}^{\infty}\int_{0}^{2\pi} \Omega \sin X \,\mathrm{d}X_0 \,\mathrm{d}Y_0 = -\frac{\mathrm{d}A}{\mathrm{d}\bar{x}}, \tag{7.11}$$

and it therefore follows from (6.35) that Ω and A can be found by solving (7.1), (7.2), (7.10) and (7.11), subject to the boundary conditions (7.3), (7.9) and

$$\Omega = (1 - r)A(\bar{x}_0)\,\mathrm{Re}\frac{\exp \mathrm{i}X_0}{Y_0 - \mathrm{i}\bar{\kappa}} \quad \text{at } \bar{x} = \bar{x}_0 \quad \text{as } \bar{x}_0 \to \infty. \tag{7.12}$$

The solutions to (7.1), (7.2) and (7.10) have the following symmetry

$$X(X_0, Y_0, \bar{x}) = -X(-X_0, -Y_0, \bar{x}), \tag{7.13}$$

$$Y(X_0, Y_0, \bar{x}) = -Y(-X_0, -Y_0, \bar{x}), \tag{7.14}$$

$$\Omega(X_0, Y_0, \bar{x}) = -\Omega(-X_0, -Y_0, \bar{x}). \tag{7.15}$$

Consequently, calculations need to be done only for $0 \leqslant Y_0 < \infty$. Rather than mapping this semi-infinite domain into a finite region, we solved (7.1), (7.2), (7.10) and (7.11) over a finite range, say $0 \leqslant Y \leqslant N$, and used the asymptotic behaviour of the solutions at $Y_0 = \infty$ to obtain an accurate approximation to the cross-stream integral in (7.11).

By using (7.1), (7.2) and (7.10) to generate asymptotic expansions it is easy to show that

$$X \to X_0 + (\bar{x} - \bar{x}_0)\, Y_0 + O\left(\frac{1}{Y_0^2}\right), \tag{7.16}$$

$$Y \to Y_0 - \frac{\sin X}{Y_0} A + \frac{\sin X}{Y_0^2} \frac{\mathrm{d}A}{\mathrm{d}\bar{x}} + O\left(\frac{1}{Y_0^3}\right), \tag{7.17}$$

$$\Omega \to (1-r) \frac{\cos X}{Y_0} A - (1-r) \frac{\sin X}{Y_0^2} \frac{\mathrm{d}A}{\mathrm{d}\bar{x}} + O\left(\frac{1}{Y_0^3}\right), \tag{7.18}$$

as $Y_0 \to \infty$. It follows that (7.11) can be approximated by

$$\left[1 - \frac{2}{N}(1-r)\right] \frac{\mathrm{d}A}{\mathrm{d}\bar{x}} = -\frac{2}{\pi} \int_0^N \int_0^{2\pi} \Omega \sin X \, \mathrm{d}X_0 \, \mathrm{d}Y_0 + O\left(\frac{1}{N^3}\right). \tag{7.19}$$

The numerical integration of (7.1), (7.2), (7.10) and (7.19) was started in the upstream linear region where (7.3), (7.9) and (7.12) provide the initial conditions. The X_0-derivative in (7.10) was discretized using a second-order central difference approximation and the trapezoidal rule was used to evaluate the integrals in (7.19). The solution was marched forward in $\bar{x}$ through a predictor–corrector procedure. A second-order Adams–Bashforth scheme was used for (7.1), (7.2) and (7.10) and a third-order scheme was used for (7.19). The combined corrector steps were then iterated until the solution at the next streamwise station had been obtained to within a preset tolerance.

As the calculation progressed into the nonlinear region, solutions to (7.1) and (7.2) for fixed values of Y_0 tended to roll up into very tight spirals resulting in a loss in grid resolution. Two steps were taken to control this loss; first, since the roll-up was most pronounced for small values of Y_0, the computational domain was decomposed into three subgrids of varying X_0 resolutions so as to provide points where they were needed most; and second, while the integration of (7.1), (7.2), (7.10) and (7.19) was being performed, mesh points along lines of constant Y_0 were redistributed by use of a cubic spline approximation whenever the spacing between adjacent points in the (X, Y)-plane exceeded a preset tolerance.

8. Numerical results and discussion

Goldstein *et al.* (1987) considered the nonlinear evolution of a two-dimensional instability wave in a weak adverse pressure gradient boundary layer. Equation (6.29) reduces to their result in the limit where $r \to 0$ and (6.29) and (6.30) become decoupled. They found that nonlinear effects always reduce the growth rate of the linear instability wave, driving it towards an equilibrium state. However, they were unable to carry their computations far enough to determine if an actual equilibrium state was achieved.

The scaled instability wave amplitude (as calculated from the present solution) is plotted as a function of the scaled and normalized streamwise coordinate $\bar{x}$ for

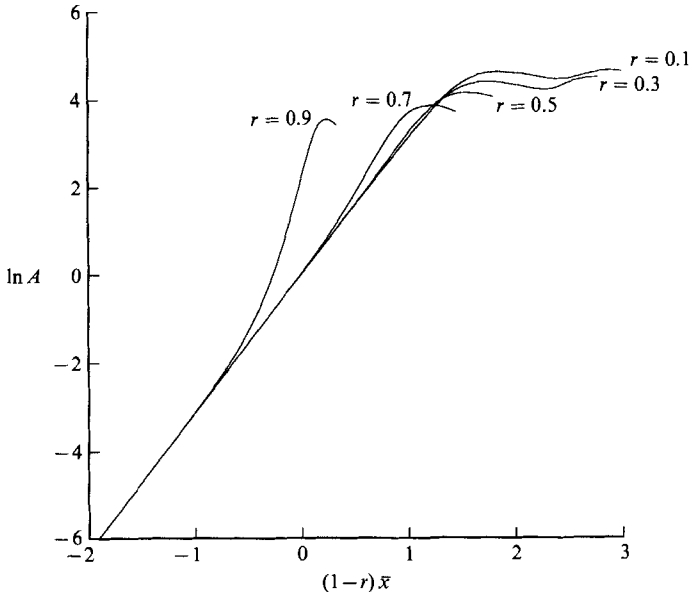

FIGURE 2. $\ln|A|$ *vs.* $(1-r)\bar{x}$ for $r = 0.1$, 0.3, 0.5, 0.7 and 0.9.

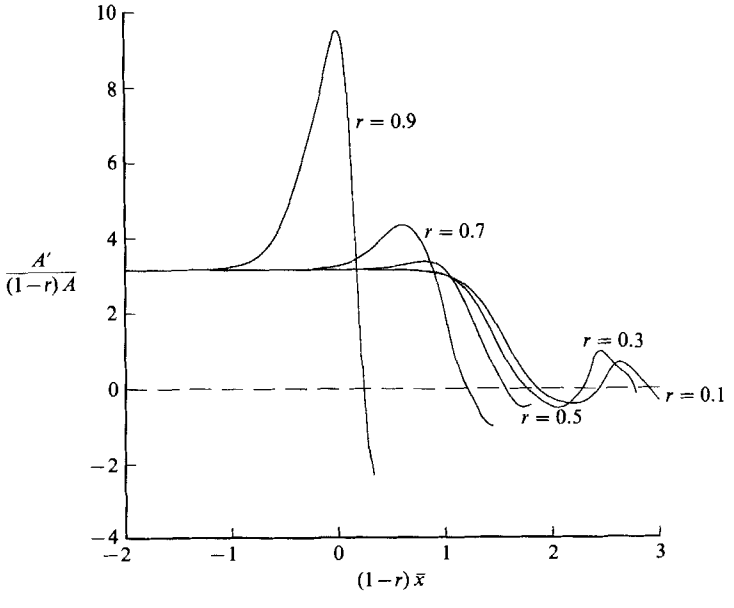

FIGURE 3. $A'/(1-r)A$ *vs.* $(1-r)\bar{x}$ for $r = 0.1$, 0.3, 0.5, 0.7 and 0.9.

various values of r in figure 2. The corresponding instability wave growth rates, $A_{\bar{x}}/A$, are shown in figure 3. As in Goldstein *et al.* (1987), the growth rates initially follow the linear growth until the amplitude becomes large enough for nonlinear effects to come into play, but now the nonlinear effects cause the growth rate to increase – presumably because compressibility effects, i.e. the Bjerknes forces, act as a vorticity source within the critical layer. Notice that the growth augmentation increases with increasing r – becoming very large as $r \to 1$. This is because the

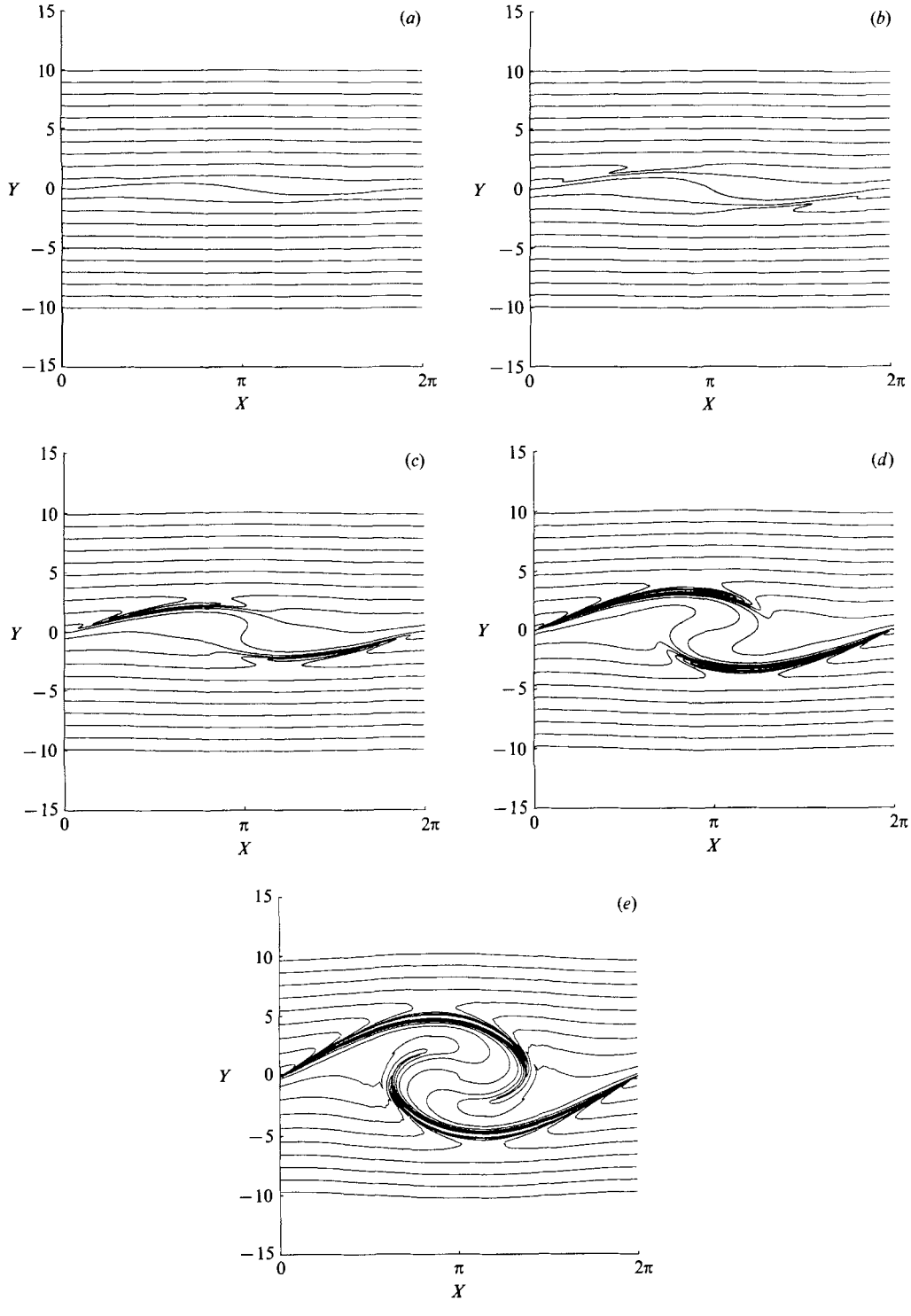

FIGURE 4. Vorticity contours in the (X, Y)-plane for $r = 0.7$ and contour values -10, -9, ..., 9, and 10: (*a*) $\bar{x} = -0$; (*b*) $\bar{x} = -0.5$; (*c*) $\bar{x} = 1.0$; (*d*) $\bar{x} = 1.5$; (*e*) $\bar{x} = 2.0$.

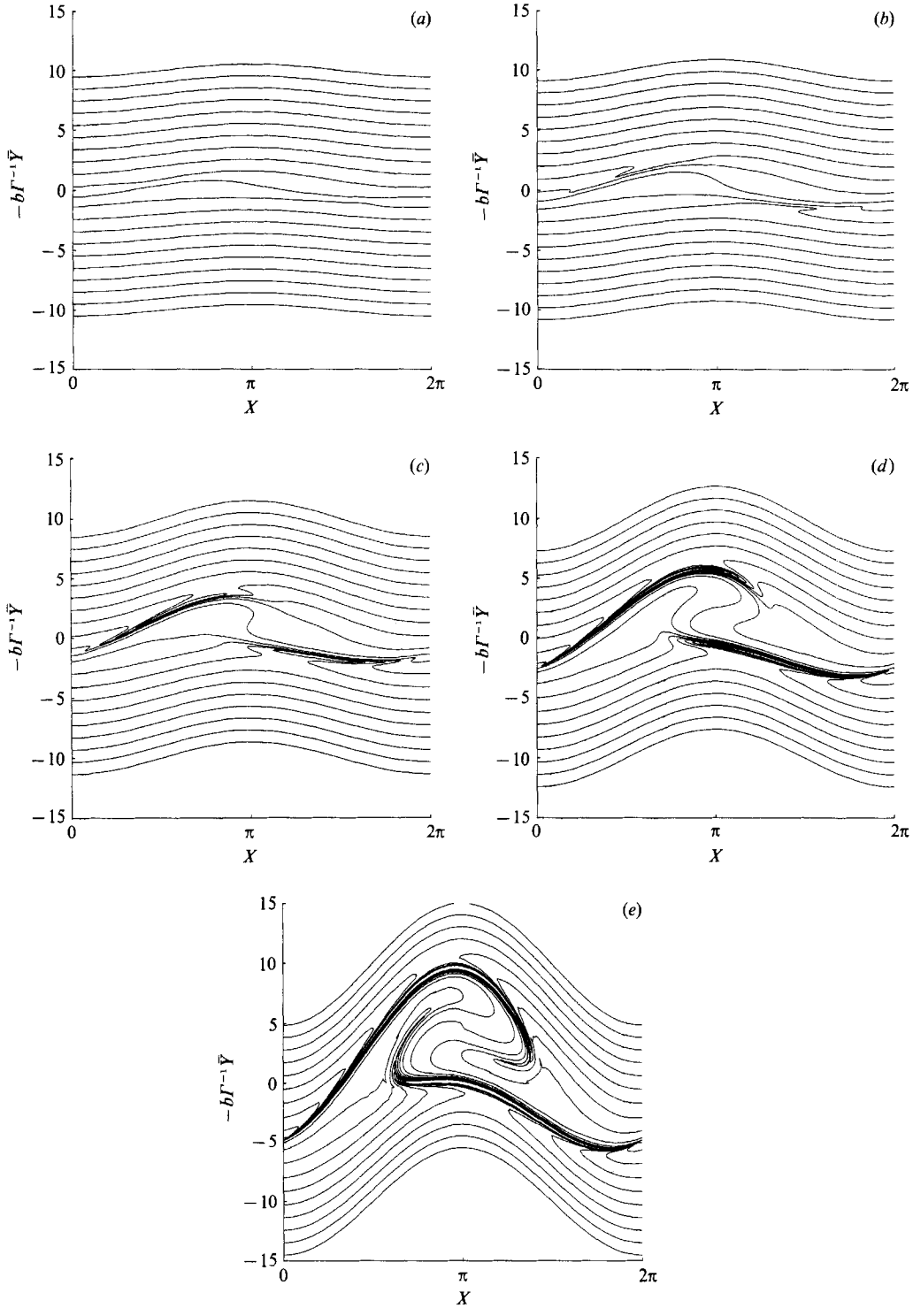

FIGURE 5. Vorticity contours in the $(X, = b\bar{Y}/\Gamma)$-plane for $r = 0.7$ and contour values -10, -9. .... 9 and 10: (a) $\bar{x} = -0$: (b) $\bar{x} = -0.5$: (c) $\bar{x} = 1.0$: (d) $\bar{x} = 1.5$: (e) $\bar{x} = 2.0$.

vorticity fluctuations become small compared to the temperature fluctuations as $r \to 1$ so that the compressible effects provide the first source of nonlinearity as the instability wave increases (as in Goldstein & Leib 1989). It is worth noting that the unnormalized linear growth rate κ determined by (4.15) is a maximum at $r \approx 0.85$.

However, transverse convection effects eventually become dominant when the continuously increasing amplitude becomes sufficiently large (as in Goldstein *et al.* 1987). The resulting nonlinear vorticity roll-up eventually reverses this initial augmentation in growth rate and eventually causes it to oscillate about zero. However, as noted in Goldstein *et al.* (1987) it is still unclear whether or not the growth rate actually goes to zero. This issue is, on the other hand, somewhat academic since, as can be seen from figure 4, the critical-layer vorticity roll-up generates progressively smaller lengthscales with increasing downstream distance, as was first noted by Stewartson (1978) for Rossby-wave critical layers. Viscous effects must then come into play and eventually determine the ultimate asymptotic state of the critical layer – as in the incompressible free-shear-flow analysis of Goldstein & Hultgren (1988). We expect the viscous effects to behave similarly in the present solution, but with vorticity/temperature coupling now playing a role in the ultimate quasi-equilibrium asymptotic solution. However, this needs to be worked out in more detail, and will be done in a forthcoming paper.

It is worth noting that the enhanced growth rates do not lead to a finite $\bar{x}$ singularly similar to the one found by Goldstein & Leib (1989) for a weakly nonlinear compressible critical layer involving temperature/vorticity coupling analogous to that of the present solution. The vorticity roll-up of the present fully nonlinear solution is apparently strong enough to reverse the growth augmentation before the singularity has had a chance to form. In fact, like the initial growth rate augmentation, the final growth rate reduction appears to increase with increasing r. It is also worth noting that the growth rate oscillations become considerably more pronounced as r approaches unity.

The improved numerical method described in §7 allowed us to carry the computations much further downstream (relatively speaking) than was heretofore possible with the previous spectral methods. The final vorticity contours of figure 4 are, therefore, much more tightly wound than the corresponding results given in Goldstein *et al.* (1987) and Goldstein & Leib (1988), but the general patterns are not all that different – the primary difference being in the contour shape between vortex cores.

However, it is important to point out that (in order to reduce the number of parameters and thereby obtain a more universal result) we plotted the present results against the transformed variable Y, which is related to the more physical scaled and shifted variable $-\bar{Y}b/\Gamma$ through (6.18) and (6.25). We therefore include figure 5, in which we replot the vorticity contours of figure 4 against the more physical coordinates X and $-\bar{Y}b/\Gamma$ for

$$\frac{\Gamma}{T_c^2 \bar{\alpha}_1 \bar{c}_1} = \tfrac{1}{2}$$

which is reasonably close to the value for the first acoustic mode with $r = 0.7$.

The resulting vorticity contours are now quite different from the previous results. Figure 5 reflects the fact that there is a superposed straining of the vorticity contours by the external instability wave velocity field (see (6.18)) which does not appear in any previous nonlinear critical-layer analysis of which we are aware. This is because

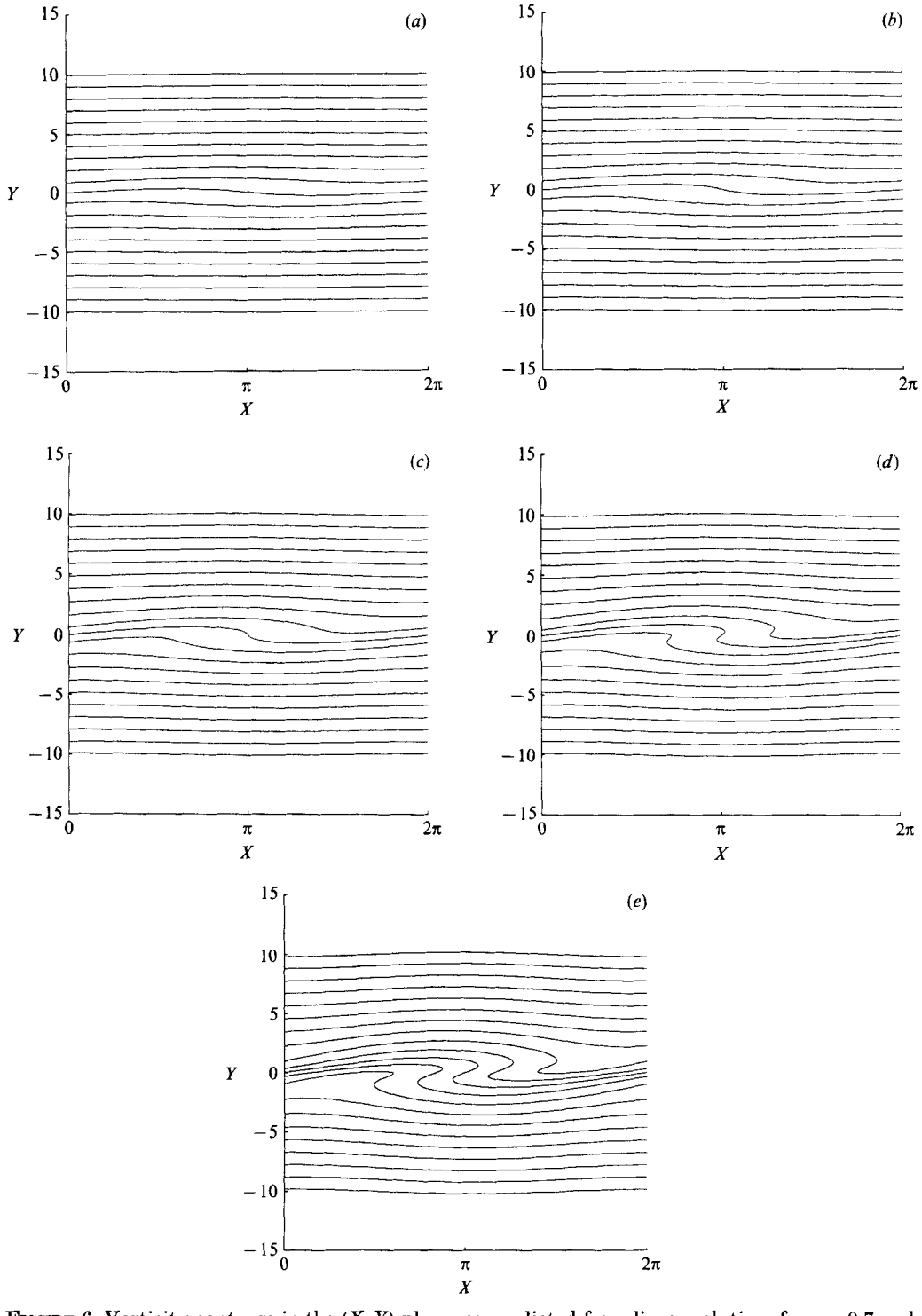

FIGURE 6. Vorticity contours in the (X, Y)-plane, as predicted from linear solution, for $r = 0.7$ and contour values -10, -9, ..., 9 and 10: (*a*) $\bar{x} = -0$; (*b*) $\bar{x} = -0.5$; (*c*) $\bar{x} = 1.0$; (*d*) $\bar{x} = 1.5$; (*e*) $\bar{x} = 2.0$.

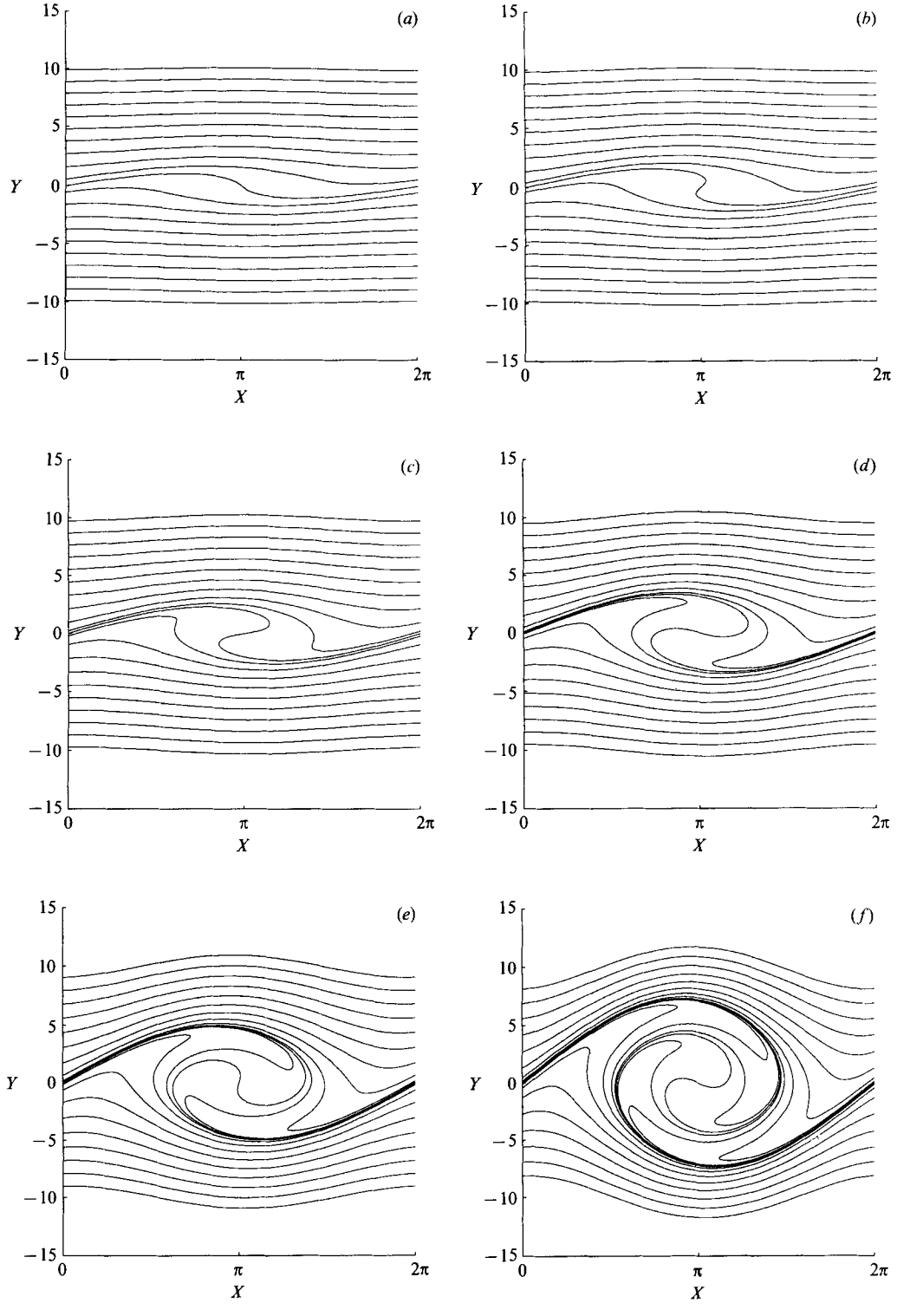

FIGURE 7(*a–e*). For caption see p. 606.

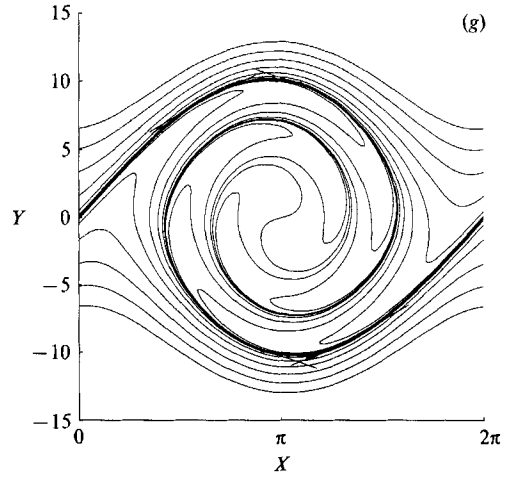

FIGURE 7. Temperature contours in the (X, Y)-plane for $r = 0.7$ and contour values -10, -9, ..., 9 and 10: (*a*) $\bar{x} = -0$; (*b*) $\bar{x} = -0.5$; (*c*) $\bar{x} = 1.0$; (*d*) $\bar{x} = 1.5$; (*e*) $\bar{x} = 2.0$; (*f*) $\bar{x} = 2.5$; (*g*) $\bar{x} = 3.0$.

the critical-layer nonlinearity is now much stronger than it was in any of these previous analyses. It is rather remarkable that this additional nonlinearity manifests itself as a simple straining of the more usual vorticity pattern (which is characterized by the simple formula (6.18)) and that this straining can have a more significant effect on the vorticity roll-up than the temperature/vorticity coupling produced by the Bjerknes force.

For the sake of comparison, we include figure 6 which shows the downstream evolution of the vorticity contours as calculated from the linear solution (6.34)–(6.37). As in the Goldstein & Leib (1988) incompressible solution the initial shearing of the constant vorticity lines is again well described by linear theory but the subsequent roll-up is not.

Finally the roll-up of the constant temperature lines is shown in figure 7 for $r = 0.7$. Notice that there is an even closer resemblance between these contours and the vorticity contours of Goldstein *et al.* (1987) than there is between the Goldstein *et al.* (1987) contours and those shown in figure 4. This is because, unlike those of Goldstein *et al.* (1987), the present vorticity contours no longer correspond to material lines (due to the Bjerknes force) while the temperature contours still retain this property.

The authors would like to thank Dr Stephen Cowley of Imperial College for helpful criticisms made in his role as a referee on the paper and for making his linear Sutherland's law solution available to us so that we could establish the viscosity law independence of the present nonlinear solution with a minimum of effort.

REFERENCES

COWLEY, S. & HALL, P. 1988 On the instability of hypersonic flow past a wedge. *ICASE rep.* 88–72.

COWLEY, S. & HALL, P. 1990 On the instability of hypersonic flow past a wedge. *J. Fluid Mech.* **214**, 17–42.

GOLDSTEIN, M. E. 1984 Aeroacoustics of turbulent shear flows. *Ann. Rev. Fluid Mech.* **16**, 263–285.

GOLDSTEIN, M. E., DURBIN, P. A. & LEIB, S. J. 1987 Roll-up of vorticity in adverse-pressure-gradient boundary layers. *J. Fluid Mech.* **183**, 325–342.

GOLDSTEIN, M. E. & HULTGREN, L. S. 1988 Nonlinear spatial evolution of an exceptionally excited instability wave in a free shear layer. *J. Fluid Mech.* **197**, 295–330.

GOLDSTEIN, M. E. & LEIB, S. J. 1988 Nonlinear roll-up of externally excited free shear layers. *J. Fluid Mech.* **191**, 481–515.

GOLDSTEIN, M. E. & LEIB, S. J. 1989 Nonlinear evolution of oblique waves on compressible shear layers. *J. Fluid Mech.* **207**, 73–96.

MACK, L. M. 1984 Boundary-layer linear stability theory. In *Special Course on Stability and Transition of Laminar Flow. AGARD Rep.* 709.

MACK, L. M. 1987 Review of linear compressible stability theory. In *Stability of Time Dependent and Spatially Varying Flows* (ed. D. L. Dwoyer & M. Y. Hussaini). Springer.

SCHLICHTING, H. 1960 *Boundary Layer Theory*. McGraw-Hill.

STEWARTSON, K. 1964 *Theory of Laminar Boundary Layers in Compressible Fluids*. Oxford University Press.

STEWARTSON, K. 1978 The evolution of the critical layer of a Rossby wave. *Geophys. Astrophys. Fluid Dyn.* **9**, 185–200.